FABRICATION OF NANOPOROUS Au-Ag THIN FILMS USING MAGNETRON SPUTTERING DEPOSITION AND ETCHING PROCESS

Bui Thi Phuong Quynh

Faculty of Chemical Engineering, Ho Chi Minh City University of Industry and Trade, Vietnam

Email: quynhbtp@huit.edu.vn

Article history

Received: 12/7/2024; Received in revised form: 25/9/2024; Accepted: 07/10/2024

Abstract

The hierarchical nanoporous structure is often described as a corrosion-derived, bi-continuous porous network of interconnected ligaments. Nanoporous metallic materials have attracted much interest as they hold great potential for advanced applications in various areas. In this study, nanoporous Au-Ag thin films were formed on the n-doped Si (110) wafers, using magnetron sputtering deposition and subsequent electrochemical etching in HF solution. The etched $Au_{0.12}Ag_{0.23}Si_{0.65}$ film had a highly rough surface, including ligaments in sizes of 30-40 nm and small pore channels with cross sizes of 10-30 nm on SEM analysis. AES depth profiling data showed that Ag atoms tended to distribute more on the surface than underlying regions after the dealloying process. The thicknesses of films before and after etching were approximately 150 nm and 100 nm, respectively. The nanoporous film exhibited a significant current response toward the electrochemical oxidation of phenol at 0.7 V. The results indicate that the as-fabricated nanoporous Au-Ag structure with the mentioned characteristics can be studied further for potential applications in chemical and biochemical areas.

Keywords: *Ag-Au system, etching, magnetron sputtering, nanoporous, thin film.*

CHẾ TẠO MÀNG MỎNG NANO XỐP Au-Ag BẰNG PHƯƠNG PHÁP PHÚN XẠ MAGNETRON KẾT HỢP VỚI KỸ THUẬT ETCHING

Bùi Thị Phương Quỳnh

Khoa Công nghệ Hóa học, Trường Đại học Công Thương Thành phố Hồ Chí Minh, Việt Nam

Email: quynhbtp@huit.edu.vn

Lịch sử bài báo

Ngày nhận: 12/7/2024; Ngày nhận chỉnh sửa: 25/9/2024; Ngày chấp nhận: 07/10/2024

Tóm tắt

Cấu trúc nano xốp hierarchy thường được nói đến như một mạng lưới xốp của các ligament gắn kết với nhau được hình thành do quá trình ăn mòn. Các vật liệu kim loại nano xốp vẫn luôn thu hút nhiều sự quan tâm vì chúng có tiềm năng lớn cho các ứng dụng tiên tiến trong nhiều lĩnh vực khác nhau. Trong nghiên cứu này, màng mỏng Au-Ag nano xốp đã được tạo thành công trên nền n-doped Si (110) wafer bằng kỹ thuật lắng đọng phún xạ magnetron và etching trong dung dịch acid HF. Màng mỏng nano xốp Au-Ag được cấu trúc từ các ligament có kích thước khoảng 30-40 nm với các lỗ xốp nhỏ dạng kênh rẽ có kích thước chiều ngang khoảng 10-30 nm. Quá trình phân tích theo chiều sâu của màng nano xốp bằng AES cho thấy rằng các nguyên tử Ag có xu hướng phân bố nhiều hơn trên bề mặt so với các lớp bên dưới. Độ dày của màng trước và sau khi xử lý ở khoảng 150 nm và 100 nm. Màng mỏng Au-Ag nano xốp cho tín hiệu dòng đáng kể đối với quá trình oxy hóa phenol khi áp một điện thế ở 0,7 V. Nghiên cứu cho thấy màng mỏng Au-Ag nano xốp đã được điều chế với những đặc tính nêu trên có thể là một chủ đề nghiên cứu đầy tiềm năng cho các ứng dụng trong các lĩnh vực hóa học và hóa sinh.

Từ khóa: *Etching, hệ Au-Ag, màng mỏng, nano xốp, phún xạ magnetron.*

DOI: https://doi.org/10.52714/dthu.14.5.2025.1404

Cite: Bui, T. P. Q. (2025). Fabrication of nanoporous Au-Ag thin films using magnetron sputtering deposition and etching process. *DongThap University Journal of Science*, *14*(5), 26-32. https://doi.org/10.52714/dthu.14.5.2025.1404.

1. Introduction

The nanoporous (NP) structure has attracted great interest owing to its distinct physical and chemical properties compared to the compact system (Kwon et al., 2024). Constructed by interconnected ligaments and nanopore channels, NP metallic thin films with large specific surface areas hold great potential applications in diverse areas, such as electrochemical sensors, optical devices, and catalysts (Kwon et al., 2024; Yuan et al., 2024). Nanoporous gold (NPG) is a three-dimensional bi-continuous NP network evolved from a corrosion or corrosion-like process. An important feature of NPG is its high surface-to-volume ratio due to a large fraction of low-coordinated surface atoms (Kim, 2018, 2021), which are normally located on terraces (CN =9), steps (CN = 7), or kink sites (CN =6). These are crucial for enhanced catalytic activity, selectivity, and optical behavior. The NPG with such a distinct structure exhibits important features, including high surface area, excellent conductivity, tunable porosity, biocompatibility, mechanical rigidity, and chemical stability (Kim, 2018; Quynh et al., 2014; Seker et al., 2009). Hence, many studies have explored its potential for applications in fuel cells, supercapacitors, batteries, electrochemical sensors, and other catalytic processes (Kim, 2021; Quynh et al., 2015; Seker et al., 2009). The unsupported dealloyed NPG was reported to demonstrate oxidation activity like supported gold nanoparticles (Fujita et al., 2012). Moreover, the NPG thin film fabricated from the Au-Si system, was found to have pronounced electrochemical activity toward several benzene derivatives (Quynh et al., 2018).

The NPG can be produced by selectively removing unwanted elements, such as Ag, Zn, and Cu out of precursor alloys. Although the commercially available Ag-rich Au-Ag alloy leaf has been commonly used, cracks and difficult pore control due to unflexible alloy compositions are the main hindrances (Wittstock et al., 2012). Under this context, methods like electrodeposition, sputtering deposition, and electron beam evaporation, have been used alternatively to form alloy thin films on a substrate followed by a dealloying process (Kim, 2018; Tran et al., 2018). This procedure has been found to form NP films with high-quality and tunable pore-related characteristics. For example, NP Au derived from an Au_xSi_{1-x}film, or NP Pt from a Pt_xSi_{1-x} film deposited by magnetron sputtering were reported to exhibit good uniformity, tunable porosity and thickness, and feasible handling (Kim, 2018; Tran et al., 2018).

To improve and expand the potential applications of NPG, several attempts have been made to develop bimetallic NP systems. Au-Ag systems have received much interest as nanosized Au and Ag may show enhanced localized surface plasmon resonance (LSPR) (Nishi et al., 2024; Yuan et al., 2024). Ai-Qin Want et al. reported the utilization of the Au–Ag alloy nanoparticles/mesoporous aluminosilicate for low-temperature CO oxidation reaction (Wang et al., 2005). Moreover, the complementary effects of Ag with Au on organic molecules and biological activities have been a topic of interest and have not been clarified yet (Yallappa et al., 2015). The fabrication of NP thin Au-Ag thin film, in which Ag composition is significant and amendable, has been rarely reported until now. Also, their synergistic chemical and biological activities are still under investigation.

This study focused on the fabrication and characterization of NP Au-Ag thin films with amendable Ag content on a Si wafer substrate. The fabrication process included two steps: magnetron sputtering deposition and electrochemical etching in HF solution. The characterization of the films was performed with SEM-EDX and AES analyses. In addition, the electrochemical behavior of the film was preliminarily evaluated through the amperometric response toward the successive addition of phenol.

2. Materials and methods

2.1. Chemicals

Sulfuric acid (>98%) was purchased from Sigma-Aldrich. Hydrofluoric acid (48.0− 51.0%) was supplied by Baker. Sodium hydroxide (>96.0%) was supplied by Xilong Ltd. and phosphate-buffered saline (PBS) pH 7.2 was supplied by Thermo-scientific. All the chemicals were used without further purification.

2.2. Fabrication of nanoporous Au-Ag thin films

Nanoporous Au-Ag (NGS) thin films were prepared by a two-step process: co-sputtering deposition of Au-Ag-Si on Si wafer substrates and wet etching in HF solution (Kim, 2018; Quynh et al., 2014). At first, in a vacuum chamber working at a base pressure of less than 2 x 10^{-6} Torr, the n-doped Si (1 1 0) substrate (1 cm × 2 cm) was coated subsequently with a Ti adhesive layer (about 5 nm) and an Au etch stop layer (about 50 nm). Then, Au, Ag, and Si were co-deposited at fixed plasma powers (10 W, DC, for Au and Ag; 200 W, RF, for Si) to receive the $Au_xAg_ySi_{1-x-y}$ films of about 150 nm. The wafers were put on a rotating disk at positions S1 and S2 as illustrated in **Figure 1**. After deposition, the back side of the sample was sealed with silicone glue before electrochemical etching in 3% HF solution under a linear potential sweep from 0 to 1.3 V at a 10 mV/s scan rate (CH660, CH Instruments Inc.). After sealing, the exposed surface for etching was 1 cm x 1cm. The electrochemical cell included a three-electrode system: Ag/AgCl (3 M KCl) as the reference electrode, Pt wire as the counter electrode, and a sealed sample as the working electrode.

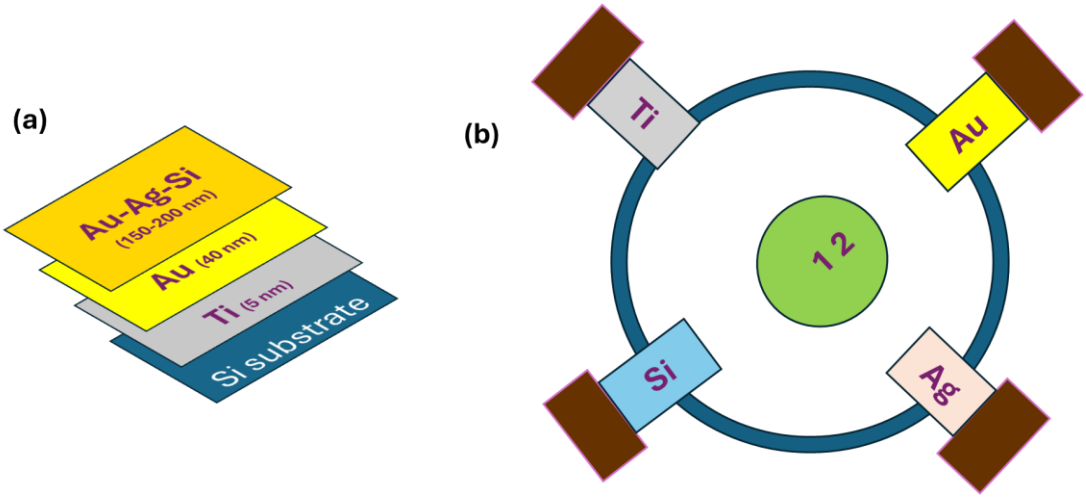

Figure 1. (a) Schematic of sputtered Au-Si films, (b) top view of the sputter positions to prepare Au-Ag thin films

2.3. Characterization of the NP Au-Ag films

The surface morphology and cross-section of the films were observed under a field-emission scanning electron microscopy (FE-SEM, SU-8220, Hitachi, High-Technologies) at a working voltage of 10 kV, coupled to an energy-dispersive X-ray spectroscopy (EDX). Depth profiling of the films was conducted on an Auger electron spectroscopy (AES) (PHI-700, Ulvac-PHI). The films were depth profiled by a 10 kV electron beam while vertically etched by a constant 3 kV Ar ion beam. The sputter time was proportional to the film depth.

The electrochemical processes were performed on a three-electrode system (CH660, CH Instruments Inc.). The Ag/AgCl (3 M KCl) electrode was used as the reference electrode, Pt wire was the counter electrode, and the NP thin film as the working electrode. The cyclic voltammogram was collected in 5 M H_2SO_4 solution under cyclic scans from −0.25 V to 1.8 V (vs Ag/AgCl) at a scan rate of 100 mV/s.

2.4. Preliminary amperometric test for phenol

Before an amperometric measurement, the NGS thin film was cleaned in 0.5 M H_2SO_4 solution under cyclic scans from −0.25 V to 1.6 V (vs Ag/AgCl) at a scan rate of 100 mV/s. Amperometric detection of phenol was conducted in a glass cell containing 10 ml of electrolyte with successive addition of phenol at a constant voltage of 0.7 V at room temperature. The phosphate-buffered saline (PBS) containing 0.15 M NaCl with pH 7.2 was used as the electrolyte. The electric currents were measured on a 1 cm × 1 cm exposed area, i.e. current densities (current/cm^2).

3. Results and discussion

3.1. Results of SEM-EDX analysis

Morphologies of Au-Ag-Si thin films before and after wet etching are presented in **Figures 2 & 3**. Before etching, the film surface was flat and contained tightly arranged grains in sizes of 20−30 nm. S1 and S2 have a similar structure, thus only the S1 surface is presented here (**Figure 2**). After etching, the granular surface evolved into a NP structure (**Figure 3**). The etched S1 has a more obvious NP structure than the etched S2. The cross-sectional view suggests that S1 is more porous and thicker than S2. According to EDX results (**Table 1**), the atomic ratios of Si and Ag in S1 are higher than those in S2, presumably due to the S2 position being close to the Au target in the vacuum chamber. The high Si content of S1 results in a porous structure of sponge-like Au-Ag ligaments (30−40 nm), which are expected to have high chemical and biochemical functions. However, since the depth penetration of EDX is up to several micrometers, much deeper than the thickness of the film, the Si content detected in EDX should include Si from the Si substrate, not only Si from the Au-Ag-Si layer.

Table 1. EDX analysis of NP Au-Ag thin films

Element	S1	S2
Au	27.86	34.01
Ag	19.62	18.94
Si	52.52	47.05
Si/Ag/Au atomic ratio	1.89/0.71/1	1.38/0.56/1

The electrochemical etching of Si in acid fluoric (HF) solution is suggested to occur via the following reactions:

Electrochemical steps:

$$Si + 2F^- \rightarrow SiF_2 + 2e^- \quad (1)$$

$$Si + 6F^- + 2H^+ \rightarrow SiF_6^{2-} + H_2 + 4e^- \quad (2)$$

$$Si + 6F^- \rightarrow SiF_6^{2-} + 4e^- \quad (3)$$

Chemical step:

$$SiF_2 + 4F^- + 2H^+ \rightarrow SiF_6^{2-} + H_2 \quad (4)$$

As Si was removed from the film, the atoms left behind would self-arrange into a new porous network; hence, a higher Si content results in a more porous structure. The leaving of Si atoms from the first atomic layer induces the remaining low-coordinated Au atoms to diffuse and form clusters on the surface (Wittstock et al., 2012). However, a high Si content may make the film more vulnerable to cracking due to the formation of large pores. That explains why several large, long pores appeared on the etched S1 surface.

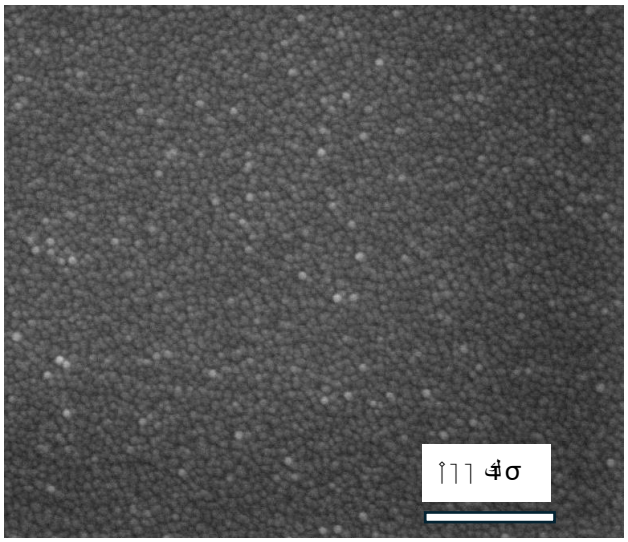

Figure 2. Surface morphology of the sputter deposited AuAgSi film (S1)

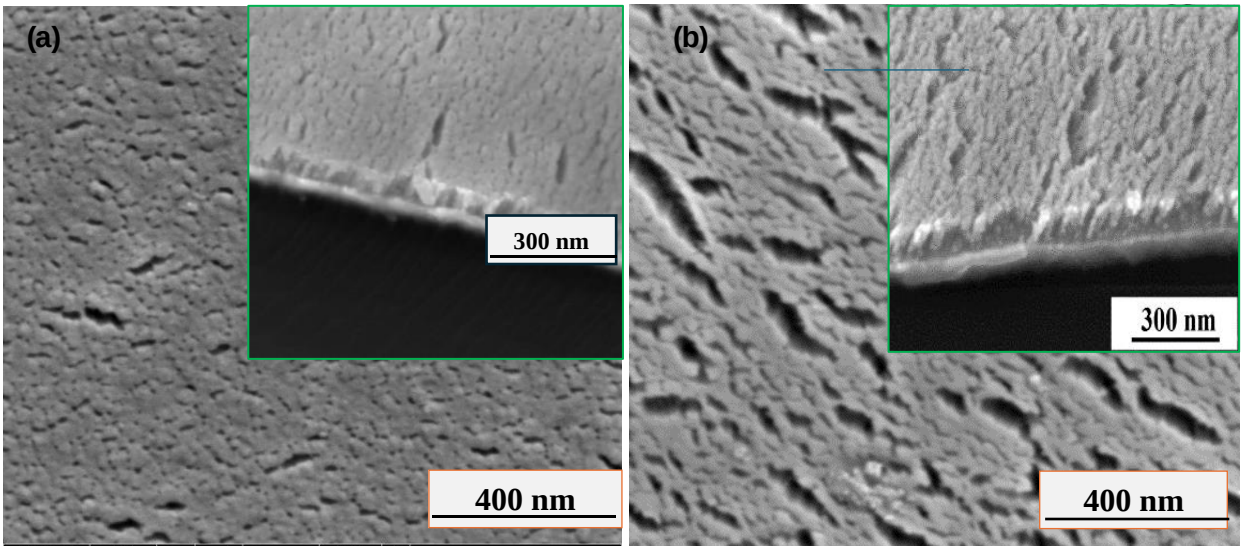

Figure 3. SEM images of the nanoporous Au-Ag thin films

3.2. AES depth profiling data

The AES depth profiles of the S1 sample, before and after etching, are presented in **Figure 4**, indicating the presence of the Au-Ag-Si layer, the Au etch stop, and the underlying Si wafer. The atom ratios of the unetched film were approximately 12% Ag, 23% Au, and 65% Si, which were the average values of the collected points during the depth profiling in the first 6 min as illustrated in Figure 4a. As calculated approximately based on the atomic etching rate, the thicknesses of films before and after dealloying were approximately 150 nm and 100 nm, respectively. The removal of Si resulted in the reconstruction of the surface structure; the surface became porous (under SEM images) and enriched in Ag elements (AES data). The Ag content was highest at the surface and decreased gradually according to the depth of the film. The sputtering time to the etch stop Au layer decreased because the film collapsed after Si was removed from the film. After dealloying, the remnant Si was detected only on very first atom layers, indicating Si was almost completely removed from the film. This is well-agreed with the previous study which reported an easy removal of Si from Au_xSi_{1-x} alloy (Gupta et al., 2012). Meanwhile, removing Si from a Pt_xSi_{1-x} system was more difficult (Jung et al., 2011). The pore size and presence of residual elements are two important factors affecting the activity of NPG, and the presence of a less-noble element normally used to form nanopores, is inevitable by dealloying technique (Fujita et al., 2012).

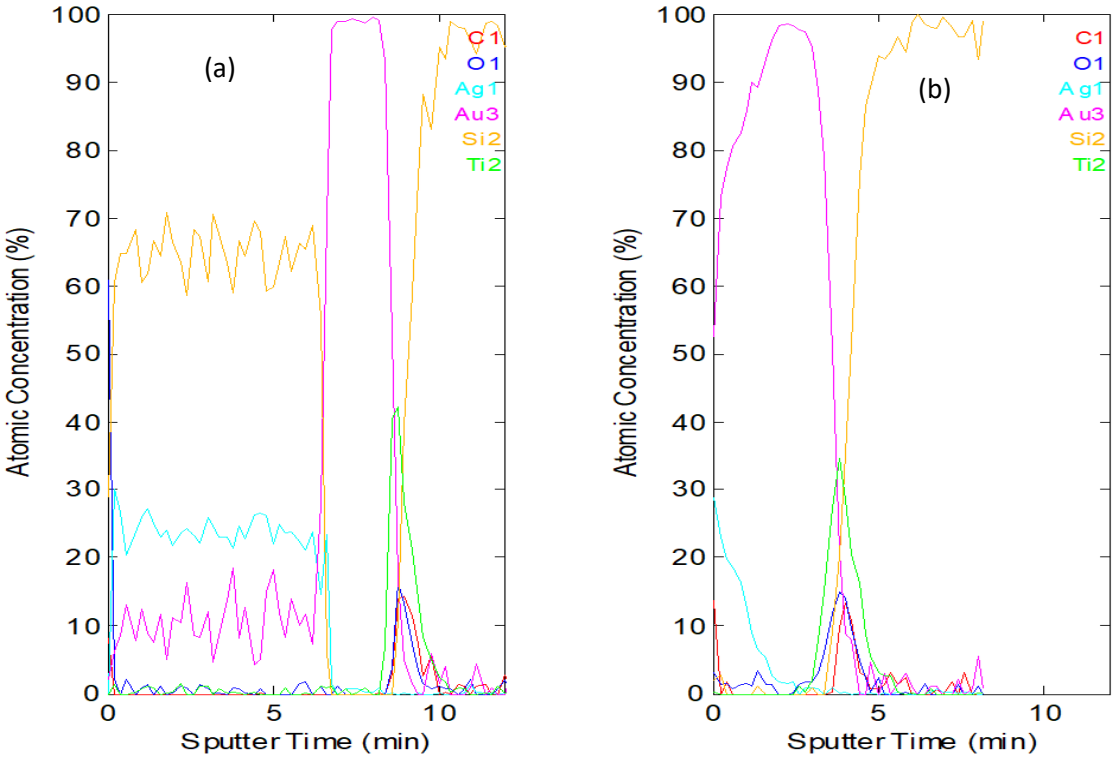

Figure 4. AES depth profiles of the $Au_{0.12}Ag_{0.23}Si_{0.65}$ thin film: (a) before dealloying, (b) after dealloying

3.3. Preliminary tests for electrochemical performance

Figure 5 illustrates a representative cyclic voltammogram of NGS (S1) in H_2SO_4 solution from -0.2 V to 1.8 V. During the positive sweep, the broad anodic peak arose from around 1.2 V to 1.5 V, revealing the formation of metal (Au, Ag) oxides before oxygen gas evolution. The peaks at about 0.9 V in the negative sweep could be attributed to the reduction of oxide layers. The flat, shallow shoulder at around 1.0 V is suggested to result from the pre-monolayer oxidation (Quynh et al., 2018). Such the voltammetric behavior of NGS may attract an interest for a potential application in catalytic electrochemical reactions.

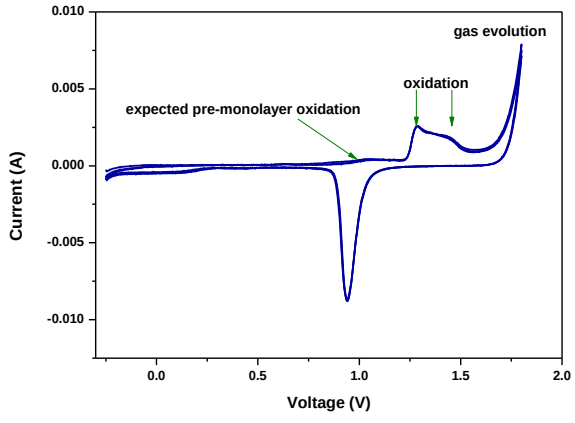

Figure 5. Cyclic voltammogram of NGS in H_2SO_4 solution

The dealloyed Au-Ag thin film (S1) exhibited a linear current response upon successive addition of phenol into PBS solution under a fixed voltage of 0.7 V **(Figure 6)**.

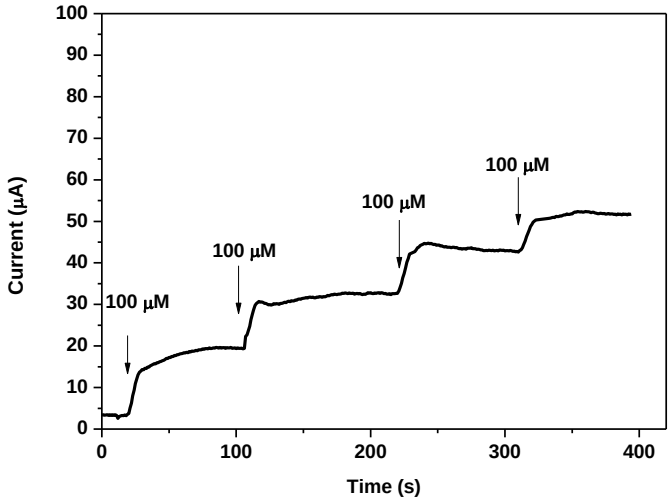

Figure 6. Current response of NGS thin film with successive addition of phenol into PBS solution at 0.7 V

The current increased 148 nA per micromole with a phenol concentration below 200 µM, and 95 nA per micromole with a phenol concentration from 200 to 400

μM. The step increase in current density in response to phenol concentration may reveal the possible application of this NP Au-Ag for sensing; however, many other factors, such as the stability of NGS structure, need further investigation. The presence of Ag in NPG thin films significantly expanded the linear detection range of the NPG only. Moreover, compared to other recently developed sensing electrodes for phenol, this NP Au-Ag shows, though lower current responses, a much broader linear range. For instance, the Tyr-CNTs-Glu/NDs-SS/GCE electrode gave a response up to 50 nm (Liu et al., 2022), and the zincon–CTAB/ SPE(Aliabadi et al., 2020) exhibits the performance in the range of 0-30 ppm.

4. Conclusions

The NP Au-Ag thin film was successfully fabricated on the silicon wafer substrate using sputtering deposition and subsequent selective wet etching. The dealloyed $Au_{0.12}Ag_{0.23}Si_{0.65}$ thin film exhibited an expected hierarchical NP structure with Au-Ag alloy ligaments. The sizes of small pore channels were in the range of 10-30 nm, while the ligaments were about 30-40 nm. The NP Au-Ag thin films were produced at relatively high quality, easily handled, and exhibited pronounced performance in preliminary electrochemical tests. The findings of this study show the possibility of fabricating NP Au-Ag thin film and its potential for applications in diverse fields, especially electrochemical and biochemical fields.

References

Fujita, T., Guan, P., McKenna, K., Lang, X., Hirata, A., Zhang, L., Tokunaga, T., Arai, S., Yamamoto, Y., Tanaka, N., Ishikawa, Y., Asao, N., Yamamoto, Y., Erlebacher, J., & Chen, M. (2012). Atomic origins of the high catalytic activity of nanoporous gold. *Nature Materials*, *11*(9), 775–780. https://doi.org/10.1038/nmat3391

Gupta, G., Thorp, J. C., Mara, N. A., Dattelbaum, A. M., Misra, A., & Picraux, S. T. (2012). Morphology and porosity of nanoporous Au thin films formed by dealloying of AuxSi1−x. *Journal of Applied Physics, 112*(9). https://doi.org/10.1063/1.4764906

Hosseini A., M., Esmaeili, N., & Samari, J., H. (2020). An electrochemical composite sensor for phenol detection in waste water. *Applied Nanoscience, 10*(2), 597–609. https://doi.org/10.1007/s13204-019-01139-6

Jung, H. Y., Kim, D. H., Chun, H. K., Kim, S. H., Lim, C. S., Byun, J. Y., & Jung, Y. J. (2011). Towards Engineering Nanoporous Platinum Thin Films for Highly Efficient Catalytic Applications. *Advanced Energy Materials*, *1*(6), 1126–1132. https://doi.org/10.1002/aenm.201100402

Kim, S. H. (2018). Nanoporous gold: Preparation and applications to catalysis and sensors. *Current Applied Physics*, 18(7), 810–818. https://doi.org/10.1016/j.cap.2018.03.021

Kim, S. H. (2021). Nanoporous Gold for Energy Applications. *The Chemical Record, 21*(5), 1199–1215. https://doi.org/10.1002/tcr.202100015

Kwon, H., Alarcón-Correa, M., Schärf, I., & Fischer, P. (2024). Ultrathin nanoporous metallic films and their integration in sensors. *Materials Advances, 5*(9), 3973–3980. https://doi.org/10.1039/D4MA00134F

Liu, Y., Chen, Y., Fan, Y., Gao, G., & Zhi, J. (2022). Development of a Tyrosinase Amperometric Biosensor Based on Carbon Nanomaterials for the Detection of Phenolic Pollutants in Diverse Environments. *ChemElectroChem, 9*(24). https://doi.org/10.1002/celc.202200861

Nishi, H., Tojo, T., & Tatsuma, T. (2024). Chiral Nanoporous Structures Fabricated via Plasmon-Induced Dealloying of Au-Ag Alloy Thin Films. *Electrochemistry, 92*(5), 1–5. https://doi.org/10.5796/electrochemistry.24-00027

Quynh, B. T. P., Byun, J. Y., & Kim, S. H. (2014). Nanoporous gold for amperometric detection of amino-containing compounds. *Sensors and Actuators B: Chemical, 193*, 1–9. https://doi.org/10.1016/j.snb.2013.11.056

Quynh, B. T. P., Byun, J. Y., & Kim, S. H. (2015). Non-enzymatic amperometric detection of phenol and catechol using nanoporous gold. *Sensors and Actuators B: Chemical, 221*, 191–200. https://doi.org/10.1016/j.snb.2015.06.067

Quynh, B. T. P., Byun, J. Y., & Kim, S. H. (2018). Electrochemical Behavior of Aromatic Compounds on Nanoporous Gold Electrode. *Journal of The Electrochemical Society, 165*(10), B414–B421. https://doi.org/10.1149/2.0411810jes

Seker, E., Reed, M. L., & Begley, M. R. (2009). Nanoporous Gold: Fabrication, Characterization, and Applications. *Materials, 2*(4), 2188–2215. https://doi.org/10.3390/ma2042188

Tran, H. T., Byun, J. Y., & Kim, S. H. (2018). Nanoporous metallic thin films prepared by dry processes. *Journal of Alloys and Compounds, 764*, 371–378. https://doi.org/10.1016/j.jallcom.2018.06.004

Wang, A.-Q., Liu, J.-H., Lin, S. D., Lin, T.-S., & Mou, C.-Y. (2005). A novel efficient Au–Ag alloy catalyst system: preparation, activity, and characterization. *Journal of Catalysis, 233*(1), 186–197. https://doi.org/10.1016/j.jcat.2005.04.028

Wittstock, A., Jürgen B., Jonah E., & Marcus B. (2012). *Nanoporous gold: from an ancient technology to a high-tech material.* Royal Society of Chemistry.

Yallappa, S., Manjanna, J., & Dhananjaya, B. L. (2015). Phytosynthesis of stable Au, Ag and Au–Ag alloy nanoparticles using J. Sambac leaves extract, and

their enhanced antimicrobial activity in presence of organic antimicrobials. *Spectrochimica Acta Part A: Molecular and Biomolecular Spectroscopy*, *137*, 236–243. https://doi.org/10.1016/j.saa.2014.08.030

Yuan, C., Zhang, D., Xu, P., & Gan, Y. (2024). Nanoporous Silver Films for Surface-Enhanced Raman Scattering-Based Sensing. *ACS Applied Nano Materials*. https://doi.org/10.1021/acsanm.4c02026